Hindawi Publishing Corporation
Advances in Power Electronics
Volume 2013, Article ID 352765, 9 pages
http://dx.doi.org/10.1155/2013/352765

Review Article

Modeling, Control, and Simulation of a Solar Hydrogen/Fuel Cell Hybrid Energy System for Grid-Connected Applications

Tourkia Lajnef, Slim Abid, and Anis Ammous

Power Electronic Group (PEG), ENIS, BP W, 3038 Sfax, Tunisia

Correspondence should be addressed to Tourkia Lajnef; lajnefturkia@yahoo.fr

Received 10 January 2013; Revised 18 February 2013; Accepted 18 February 2013

Academic Editor: Jose Pomilio

Different energy sources and converters need to be integrated with each other for extended usage of alternative energy, in order to meet sustained load demands during various weather conditions. The objective of this paper is to associate photovoltaic generators, fuel cells, and electrolysers. Here, to sustain the power demand and solve the energy storage problem, electrical energy can be stored in the form of hydrogen. By using an electrolyser, hydrogen can be generated and stored for future use. The hydrogen produced by the electrolyser using PV power is used in the FC system and acts as an energy buffer. Thus, the effects of reduction and even the absence of the available power from the PV system can be easily tackled. Modeling and simulations are performed using MATLAB/Simulink and SimPowerSystems packages and results are presented to verify the effectiveness of the proposed system.

1. Introduction

At present, most of energy demand in the world relies on fossil fuels such as petroleum, coal, and natural gas that are being exhausted very fast. One of the major severe problems of global warming is one of these fuels combustion products, carbon dioxide; these are resulting in great danger for life on our planet [1].

Fossil fuels can have as an alternative some renewable energy sources like solar, wind, biomass, and so; among them on the photovoltaic (PV) generator which converts the solar radiation into electricity, largely used in low power applications. The photovoltaic generator is chosen for its positive points including being carbon free and inexhaustible; moreover, it does not cause noise for it is without moving parts and with size-independent electric conversion efficiency [2].

Nevertheless, the power generated by a PV system is influenced by weather conditions; for example, at night or in cloudy periods, it would not generate any power or application. In addition, it is difficult to store the power generated by a PV system for future use. The best method to overcome this problem is to integrate the PV generator with other power sources such as an electrolyser, hydrogen storage tank, FC system, or battery due to their good features such as high efficiency response, modular production, and fuel flexibility [3, 4]. Its coordination with a PV system could be successful for both grid-connected and stand-alone power applications. Thanks to the rapid response capability of the fuel cell power system, the photovoltaic fuel cell hybrid system can be able to overcome the inconvenience of the intermittent power generation. Furthermore, unlike a secondary battery, the FC does not only store energy but also produce electricity for unlimited time to support the PV power generator. Hence, the coordination between the FC power system and the photovoltaic generator becomes necessary in order to smooth out the PV power fluctuations.

This paper focuses on developing a simulation model to design and size the hybrid system for a variety of loading and meteorological conditions. This simulation model is performed using Matlab and SimPowerSystems and results are presented to verify the effectiveness of the proposed system.

2. Modeling

2.1. A Dynamic Model of PV Generator. PV arrays are built up with combined series/parallel combinations of PV solar cells, which allow extracting the characteristic parameters of the one-diode equivalent model for a single solar cell.

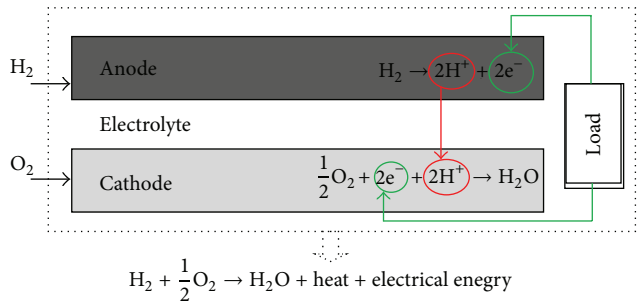

Figure 1: Cross-sectional view of a PEMFC.

The PV cell output voltage is a function of the photocurrent that is mainly determined by load current depending on the solar irradiation level during the operation [2]:

$$V_{\mathrm{PV}} = \frac{N_s kT}{q} \ln\left[\frac{I_{\mathrm{sc}} - I_{\mathrm{PV}} + I_0 N_p}{N_p I_0}\right] - \frac{N_s}{N_p} R_s I_{\mathrm{PV}}. \quad (1)$$

The parameters used in the mathematical model of the PV system are shown in the abbreviations section.

2.2. A Dynamic Model of PEMFC. The PEMFC is an electrochemical device which allows the electric energy conversion of the chemical energy contained in a reaction between a fuel, the hydrogen, and an oxidizer, the oxygen. The temperature effects have been taken into account in the typical range of low temperature PEM (60–100°C) and a thermal behaviour submodel has been introduced.

A bias voltage is applied across the electrochemical cell in order to induce electrochemical reactions at both electrodes. Water is introduced at the anode and dissociated into oxygen, protons, and electrons. The protons are driven by an electric field through the PEM to the cathode where they combine with the electrons arriving from the external circuit to form hydrogen gas. The assessment of these two half reactions produces water, heat, and electricity as Figure 1 shows.

Many models have been proposed to simulate the fuel cell in the literature [4, 5]. This model is built by utilizing the relationship between the output voltage and potential pressure of hydrogen, oxygen, and water. Figure 2 shows the detailed PEMFC model, which is then embedded into the SimPowerSystems of MATLAB-controlled voltage source and integrated into the overall system.

The proportional relationship of the molar flow of gas through a valve with its partial pressure can be expressed as

$$\frac{q_{\mathrm{H_2}}}{P_{\mathrm{H_2}}} = \frac{K_{\mathrm{an}}}{\sqrt{M_{\mathrm{H_2}}}} = K_{\mathrm{H_2}}. \quad (2)$$

For hydrogen molar flow, the derivative of the partial pressure can be calculated using the perfect gas equation as follows [5]

$$\frac{d}{dt} P_{\mathrm{H_2}} = \frac{RT}{V_{\mathrm{an}}}\left(q_{\mathrm{H_2}}^{\mathrm{in}} - q_{\mathrm{H_2}}^{\mathrm{out}} - q_{\mathrm{H_2}}^{r}\right). \quad (3)$$

The relationship between the hydrogen flow and the FC system current can be written as [5]

$$q_{\mathrm{H_2}}^{r} = \frac{N_0 I}{2F} = 2K_r I. \quad (4)$$

Using (4) and (3), the hydrogen partial pressure can be rewritten in the (s) domain as [5]

$$P_{\mathrm{H_2}} = \frac{1/K_{\mathrm{H_2}}}{1 + \tau_{\mathrm{H_2}} s}\left(q_{\mathrm{H_2}}^{\mathrm{in}} - 2K_r I\right), \quad (5)$$

where

$$\tau_{\mathrm{H_2}} = \frac{V_{\mathrm{an}}}{K_{\mathrm{H_2}} RT}. \quad (6)$$

Typically, the fuel cell output voltage is obtained from the sum of three effects [5, 6], the Nernst potential, the cathode and anode activation overvoltage, and the ohmic overvoltage due to internal resistance:

$$V_{\mathrm{cell}} = E + \eta_{\mathrm{act}} + \eta_{\mathrm{ohmic}}, \quad (7)$$

where

$$\eta_{\mathrm{act}} = -B \ln(CI), \qquad \eta_{\mathrm{ohmic}} = -R^{\mathrm{int}} I. \quad (8)$$

Now, the Nernst voltage in terms of gas molarities may be expressed as [5]

$$E = N_0\left[E_0 + \frac{RT}{2F}\log\left[P_{\mathrm{H_2}} P_{\mathrm{O_2}}^{0.5}\right]\right]. \quad (9)$$

The FC system consumes hydrogen obtained from the on-board high-pressure hydrogen tanks according to the power demand. A feedback control strategy is used to control hydrogen flow rate according to the output power of the FC system. This feedback control is achieved where FC current how the output is taken back into the input while converting the hydrogen into molar form [5, 7].

The quality of hydrogen found from the hydrogen tank is given by:

$$q_{\mathrm{H_2}}^{\mathrm{req}} = \frac{N_0 N_s I}{2FU}. \quad (10)$$

2.3. An Electrolyser Model. Electrolysis of water is the dissociation of water molecules into hydrogen and oxygen gas. The electrochemical reaction of water electrolysis is given by

$$\mathrm{H_2O_{(liquid)}} + \text{electrical energy} \Longrightarrow \mathrm{H_{2(gas)}} + \frac{1}{2}\mathrm{O_2}. \quad (11)$$

The rate of hydrogen reacting is directly proportional to the electrical current in the equivalent electrolysis circuit [8, 9], given by

$$n_{\mathrm{H_2}} = \frac{\eta_F n_c i_e}{2F}. \quad (12)$$

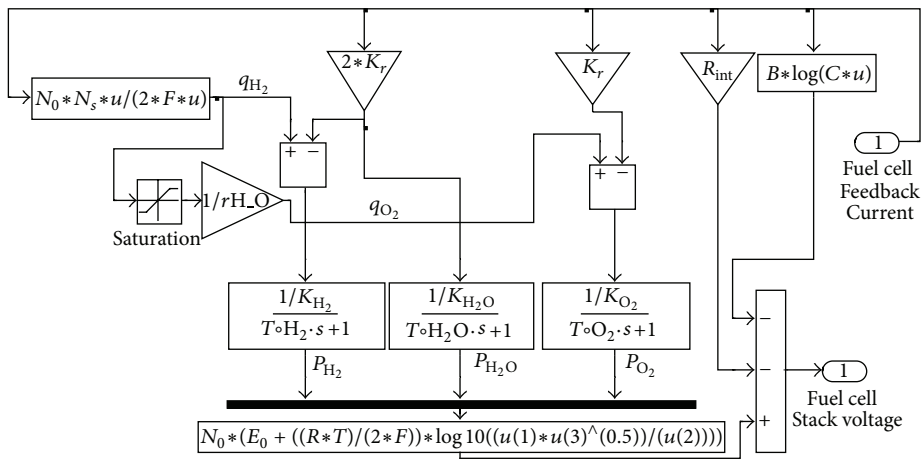

Figure 2: Dynamic model of the FC system.

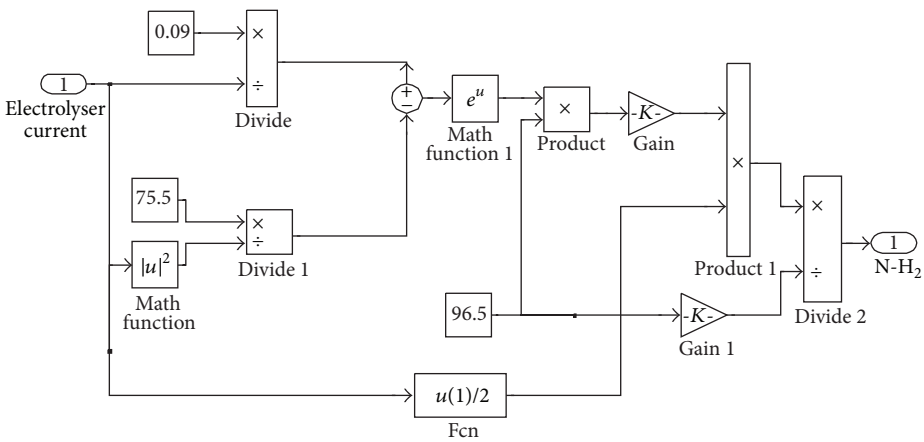

Figure 3: The Simulink diagram of the electrolyser model.

The relation between the real hydrogen flow rate and the theoretical one is defined as the Faraday's efficiency. In general, it is assumed to be more than 99%. The Faraday efficiency is expressed by [9, 10]

$$\eta_F = 96.5e^{(0.09/i_e - 75.5/i_e^2)}. \tag{13}$$

Figure 3 shows the simulation model of the electrolyser implemented in MATLAB/Simulink.

2.4. A Hydrogen Storage System. The amount of hydrogen required by the PEMFC is sent directly from the electrolyzer system based on the relationship between the output power and the hydrogen requirement of the PEMFC system. The remaining amount of hydrogen is sent to the storage tank [11]. The parameters used in the hydrogen storage system are listed in the abbreviations section.

In this study, the dynamic of the storage is obtained as follows [10, 11]:

$$\widehat{P_b - P_{bi}} = Z\frac{N_{H_2} R T_b}{M_{H_2} V_b}. \tag{14}$$

Neither the compression dynamics nor the compression energy requirements are accounted for in our calculations. All auxiliary power requirements such as pumps, valves were ignored in the dynamic model. The Simulink version of the hydrogen storage model is depicted in Figure 4.

2.5. An Averaged Model of the Converters. The simulation of power electronic systems behavior using semiconductor refined models gives an accurate, but unaffordable results. The structure of the switch cell is given in Figure 5; it has two basic switching cells (P-cell and N-cell).

Each cell consists of one controlled switch and one diode. The two active switches are directly controlled by external control signals. The diodes are indirectly controlled by the state of the controlled switches and the circuit conditions. The load is presented by an inductor L and a voltage source (V_s). The DC loop inductance is modeled by an inductor L_{st}. Depending on the sign of the load current $I_L(t)$, only two devices (one controlled device and one diode) operate simultaneously [12–15].

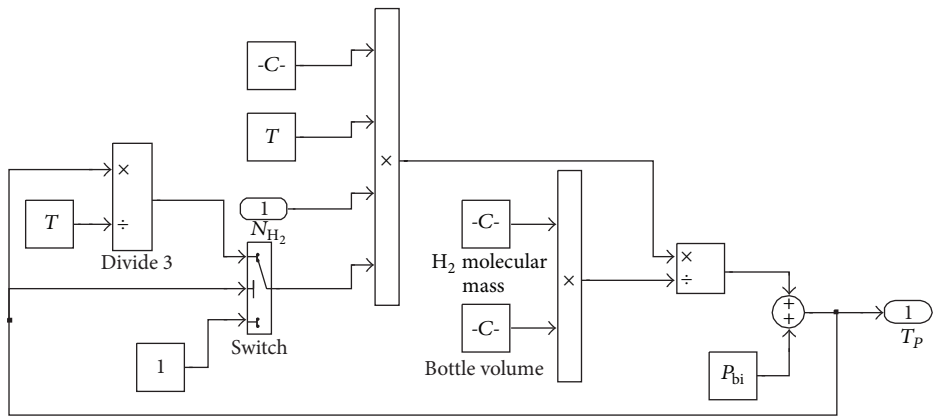

Figure 4: The Simulink model of the hydrogen storage system.

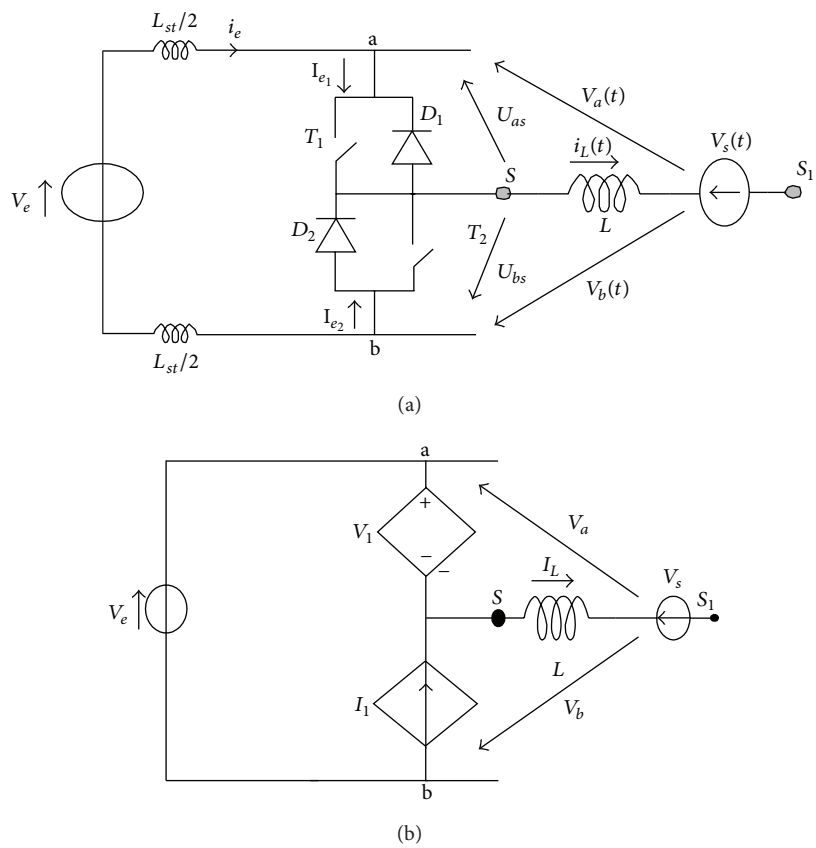

Figure 5: (a) The PWM switch, (b) the equivalent circuit of the PWM switch averaged model.

The proposed averaged model of the PWM-switch is presented in Figure 5(b). This model contains a controlled voltage source (V_1) and a controlled current source (I_1). The PWM-switch is the only nonlinear element which is supposed to be responsible for the nonlinear behavior of the converter, Considering T_s as the switching period of the controlled switches and (d) the duty ratio which is the ratio of the on-time value (T_{on}) of the upper controlled switch (T_1) and the switching period T_s.

In Figure 5(b), the current source (I_1) and the voltage source (V_1) are given by

$$V_1 = \langle V_{as} \rangle, \qquad I_1 = \langle i_{e_2} \rangle, \tag{15}$$

where $\langle U_{as} \rangle$ and $\langle i_{e_2} \rangle$ are the time averaged values of the instantaneous terminal waveforms $U_{as}(t)$ and $i_{e_2}(t)$, respectively, over one cycle T_s.

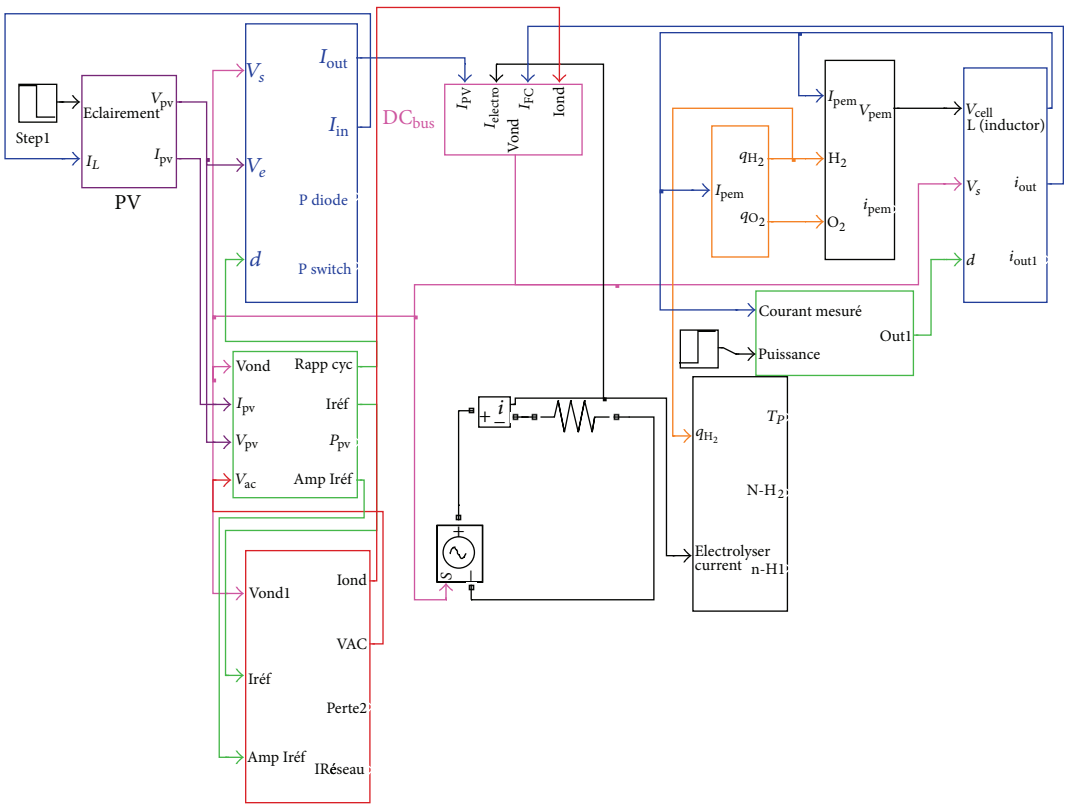

Figure 6: Schematic drawing of the PVFC hybrid system.

In this paper we have chosen MOSFET's devices for the controlled switch and the PIN devices for diodes. We notice that the load current i_L is considered constant and equal to the averaged value of the real current $i_L(t)$ in the load over the switching period T_s. During devices turn-on and turn-off phases, the different voltage magnitudes are given by

$$V_x = -\left(L_{st}\left(\frac{dI_F}{dt} + \frac{dI_R}{dt}\right) - V_d\right),$$
$$V_{\mathrm{RM}} = -\left(V_e + L_{st}\frac{dI_R}{dt} - V_t\right), \qquad (16)$$
$$V_{st} = L_{st}\frac{dI_F}{dt}, \qquad V_q = V_e + V_d - L_{st}\frac{dI_F}{dt}.$$

The averaged values of the voltage across the device of the voltage source V_1 and current I_1 are obtained by integrating the voltage and the current evolutions over one cycle T_s.

2.6. The PV System Model and Integration to the Overall Hybrid Model. As shown in Figure 6, the majority of the PVFC system comprises a solar-cell model, a PEM fuel cell generator, and a water electrolyser. The parameters of the PV systems are listed in Table 1. The PEMFC system parameters are given in Table 2.

DC-DC converters are widely used in PV generating systems as an interface between the PV generator and the water electrolyser. An optimized controller for the DC-DC must find the optimum duty cycle which leads the PV generator as close as possible to its MPPT and ensure that the working point at the water electrolyser is a safety point. Since the fuel cell stack operates at a low DC voltage range (102 V in this paper), the DC-DC converter must boost the DC voltage and invert it to the AC grid frequency (230 V/50 Hz here) for grid-connected operations. To keep the DC buses fixed at 400 V, we chose to use a hysteresis regulator.

Hence, the fuel cell control problem is translated into an output current control requirement, to be realized by the DC/DC converter, in order to ensure optimal operation for

Table 1: PV system model parameters.

PV system model parameters	Value
The number of parallel cells per strings (N_p)	36
The number of series cells per strings (N_s)	1
The number of parallel modules	6
Ideality or completion factor (a)	1.9
Boltzmann's constant (k)	1.3805e − 23 [j/°K]
PV cell temperature (T)	298 [°K]
Electron charge (q)	1.6e − 19C
Short-circuit cell current (representing insolation level) (I_{sc}) (A)	2.926
PV cell reverse saturation current (I_0) (A)	0.00005
Series resistance of PV cell (R_s) (Ω)	0.0277

Table 2: FC system model parameters.

FC system model parameters	Value
Activation voltage constant (B)	0.04777 [A^{-1}]
Activation voltage constant (C)	0.0136
Conversion factor (CV)	2
Faraday's constant (F)	96484600 [C/kmol]
Hydrogen time constant (τ_{H_2})	3.37 [s]
Hydrogen valve constant (K_{H_2})	$4.22 * 10^{-5}$ [kmol/(atms)]
Hydrogen-oxygen flow ratio (r_{H-O})	1.168
K_r constant = $N_0/4 * F$	$2.2802 * 10^{-7}$ [kmol/(atms)]
Number of cells (N_0)	88
Number of stacks (N_s)	1
Oxygen time constant (τ_{o_2})	6.74 [s]
Oxygen valve constant (K_{o_2})	$2.11 * 10^{-5}$ [kmol/(atms)]
FC system internal resistance (R_{int})	0.00303 (Ω)
FC absolute temperature (T)	343 [K]
Universal gas constant (R)	8314.47 [j/(kmol K)]
Utilization factor (U)	0.8
Water time constant (τ_{H_2O})	18.418 [s]
Water valve constant (K_{H_2O})	$7.716 * 10^{-6}$ [kmol/(atms)]

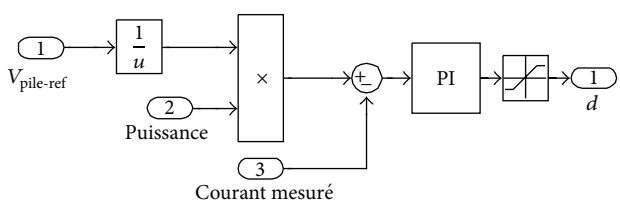

Figure 7: Inner control loop insuring fast dynamics of PEMFC.

a given fuel flow rate. Under these conditions, the cell output power is directly related to its fuel consumption at the selected optimum operating point of the V-I characteristic.

Operating the fuel cell at different output power levels requires suitable variation of its input flow rate, to be realized by the overall control system of the cell. The power demand requirement of the fuel cell is translated into a current demand input by dividing with stack output voltage:

$$I_{demand} = \frac{P_{demand}}{V_{fc}}. \quad (17)$$

2.7. Control Strategy of the Hybrid Power System. The proposed control strategy is based on a power decoupling strategy in the frequency domain of the power source. This energy-management strategy fulfills the fast energy demands if the load respects the integrity of each source. The inner control loop is tuned to drive the PEMFC current. V_{Bus} can be considered constant during current regulation. With this assumption, a classical proportional-integral (PI) controller is proposed (Figure 7).

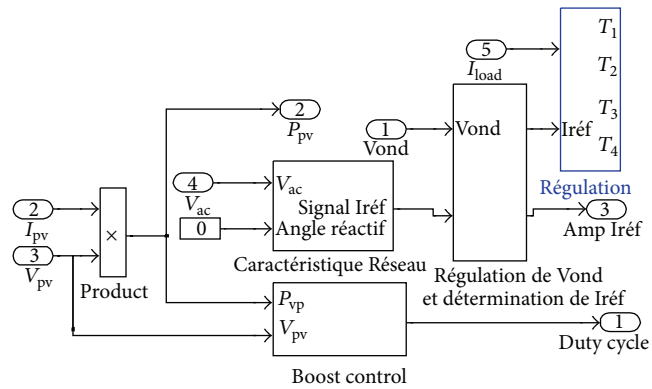

Figure 8: Current regulation implementation.

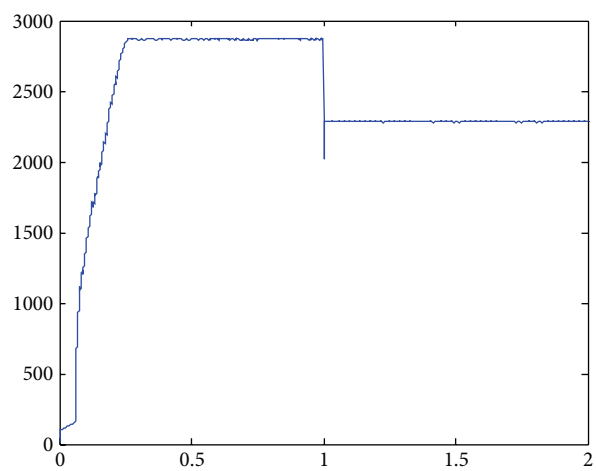

Figure 9: Power drawn from solar system.

The implementation structure of the loop regulation with hysteresis is given in Figure 8 scheme. This cascaded control structure shows that it could satisfy the different requirements of the hybrid system both from the point of view of the feed load and from the point of view of the component limits.

3. Results and Discussion

In this section we present simulation results for the coupling between the PV/FC and the PEM electrolyser through the DC-DC converter controller. The PV generator is a 2880 W power plant at 1000 (w/m^2) solar radiation. From Figures 9 and 10, we observe that the current and the available power from the PV generator decreases because of radiation variation.

Initially, the total power generated by the PV generator is sent to the electrolyser through a DC-DC converter to generate hydrogen. The hydrogen produced by the electrolyser causes the pressure of the storage tank to vary as shown in Figure 11. These results are obtained for two values of solar radiation 1000 (w/m^2) and 800 (w/m^2). We notice that the final value of pressure is used as initial condition in the following simulation.

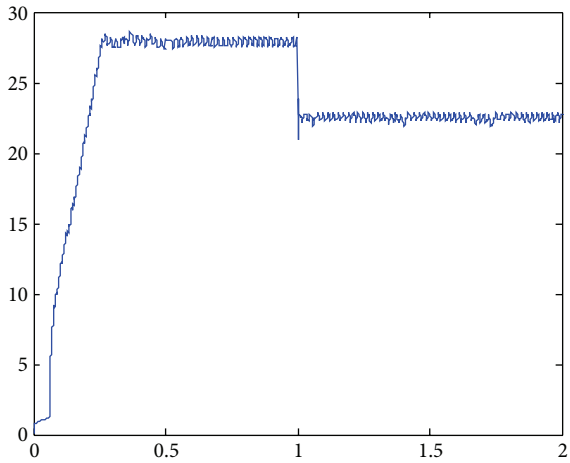

Figure 10: The current variation for the PV solar system.

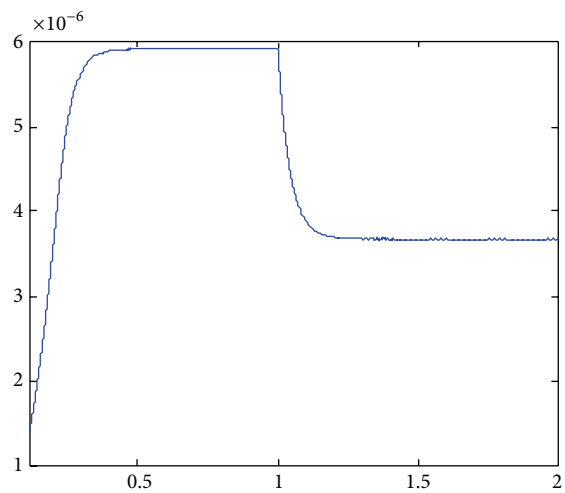

Figure 11: Amount of hydrogen produced by electrolyser.

After this, the total power generated by the PV system is sent to grid via a DC/AC converter. At 1000 (w/m^2) solar radiation, the PV generator used in this study is capable of delivering 2880 W while the FC delivers 200 W, but at 800 (w/m^2) solar radiation (at 1 s) the power produced by the PV system tends to 2300 W. So the generated power by the PV is less than the demand; power will be supplied from the FC system. The power produced by the FC system tends to 500 W at 1 s of time simulation.

The internal voltage of the FC system decreases when the FC output power increases. This relation between power and the voltage of the FC system authenticates the reliability of the FC model. The transient response of the FC system voltage to the load changes varies according to the amount of power supplied by the FC system as shown in Figure 12. The power produced by the FC system is given in Figure 13.

The amount of hydrogen moles consumed by the FC system is proportional to the power drawn from the FC system. The hydrogen flow to the FC system per second is depicted in Figure 14.

Figure 15 shows the hydrogen storage tank pressure variation corresponding to the amount of hydrogen extracted

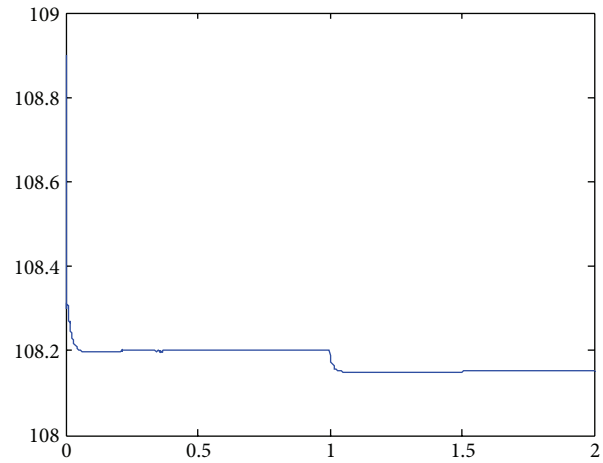

Figure 12: Voltage of the fuel cell.

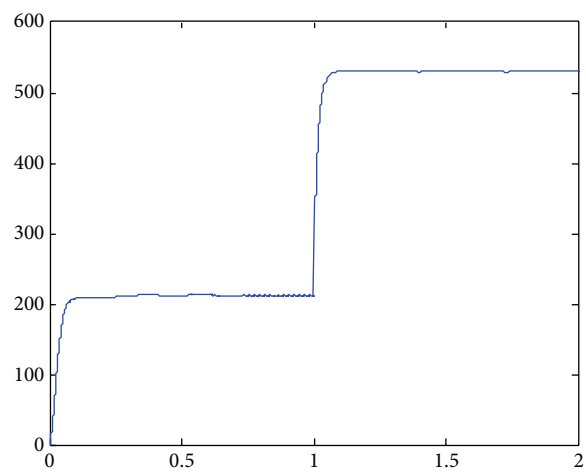

Figure 13: Power produced by the FC system.

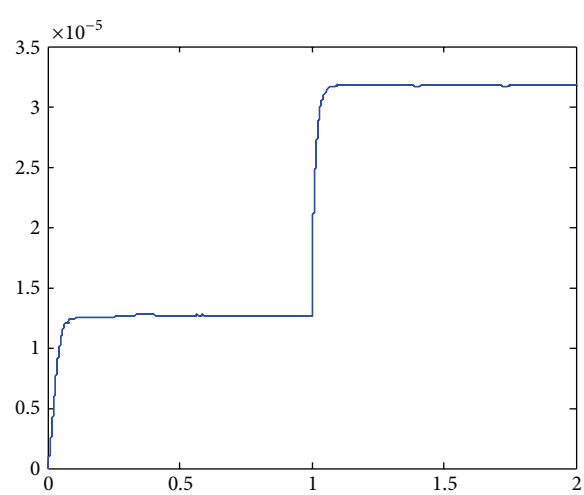

Figure 14: The molar flow of hydrogen consumed by FC.

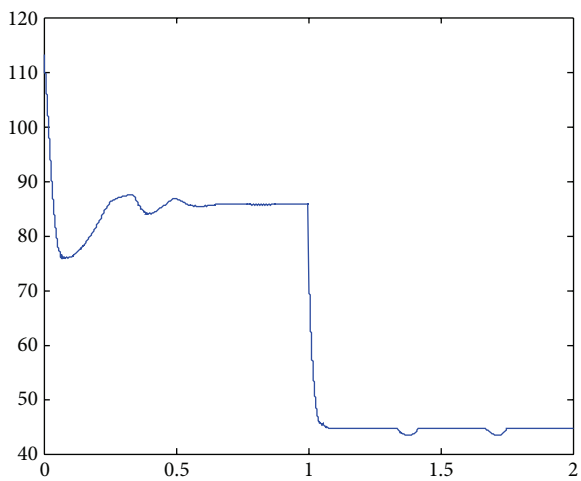

Figure 15: The pressure variation of the hydrogen storage tank.

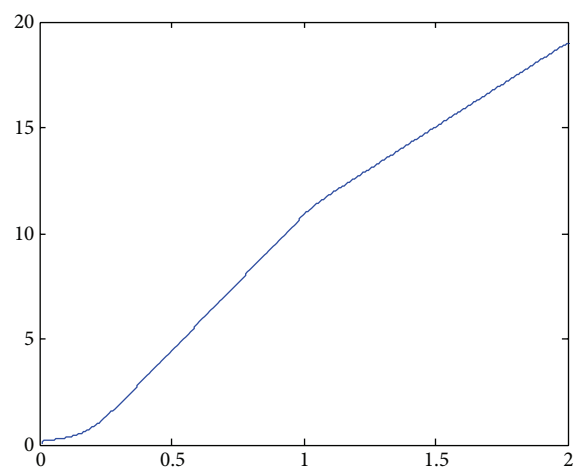

Figure 16: The pressure variation of storage hydrogen.

from the storage tank. It is evident that the hydrogen storage tank pressure decreases with time as more and more hydrogen is extracted from the storage tank. The pressure variation of storage hydrogen is as illustrated in Figure 16.

4. Conclusion

In this paper, a PV/FC generator and PEM electrolyser have been described for a PV/FC system intended for grid-connected operations. Special attention has been paid to the modeling of temperature dependence, concentration over potential, and limiting current in the PEM electrolyser model. Then, the power conditioning system, including the DC/DC and DC/AC converters, is presented and typical waveforms are shown from its simulation in MATLAB/Simulink.

Abbreviations

a: Ideality or completion factor
I_0: PV cell reverse saturation current [A]
I_{PV}: PV cell output current [A]
I_{sc}: Short-circuit cell current (representing insolation level [A])
k: Boltzmann's constant [j/°K]
M_v: Voltage factor
N_p: The number of parallel strings
N_s: The number of series cells per string
q: Electron charge [C]
R_s: Series resistance of PV cell [Ω]
T: PV cell temperature [°K]
V_{MP}: PV cell voltage corresponding to maximum power [V]
V_{oc}: Open-circuit voltage [V]
V_{PV}: Terminal voltage for PV cell [V]
M_{H_2}: Molar mass of hydrogen [kg kmol^{-1}]
N_{H_2}: Hydrogen moles per second delivered to the storage tank [kmol/s]
P_b: Pressure of tank [pascal]
P_{bi}: Initial pressure of the storage tank [pascal]
R: Universal (Rydberg) gas constant [j/(kmol K)]
T_b: Operating temperature [°K]
V_b: Volume of the tank [m^3]
Z: Compressibility factor as a function of pressure.

References

[1] K.-S. Ro and S. Rahman, "Two-loop controller for maximizing performance of a grid-connected photovoltaic-fuel cell hybrid power plant," *IEEE Transactions on Energy Conversion*, vol. 13, no. 3, pp. 276–281, 1998.

[2] Y. Sukamongkol, S. Chungpaibulpatana, and W. Ongsakul, "A simulation model for predicting the performance of a solar photovoltaic system with alternating current loads," *Renewable Energy*, vol. 27, no. 2, pp. 237–258, 2002.

[3] J. J. Hwang, D. Y. Wang, N. C. Shih, D. Y. Lai, and C. K. Chen, "Development of fuel-cell-powered electric bicycle," *Journal of Power Sources*, vol. 133, no. 2, pp. 223–228, 2004.

[4] J. J. Hwang, W. R. Chang, F. B. Weng, A. Su, and C. K. Chen, "Development of a small vehicular PEM fuel cell system," *International Journal of Hydrogen Energy*, vol. 33, no. 14, pp. 3801–3807, 2008.

[5] M. Y. El-Sharkh, A. Rahman, M. S. Alam, P. C. Byrne, A. A. Sakla, and T. Thomas, "A dynamic model for a stand-alone PEM fuel cell power plant for residential applications," *Journal of Power Sources*, vol. 138, no. 1-2, pp. 199–204, 2004.

[6] J. Padullés, G. W. Ault, and J. R. McDonald, "Integrated SOFC plant dynamic model for power systems simulation," *Journal of Power Sources*, vol. 86, no. 1, pp. 495–500, 2000.

[7] J. Hamelin, K. Agbossou, A. Laperrière, F. Laurencelle, and T. K. Bose, "Dynamic behavior of a PEM fuel cell stack for stationary applications," *International Journal of Hydrogen Energy*, vol. 26, no. 6, pp. 625–629, 2001.

[8] M. J. Khan and M. T. Iqbal, "Dynamic modeling and simulation of a small wind-fuel cell hybrid energy system," *Renewable Energy*, vol. 30, no. 3, pp. 421–439, 2005.

[9] O. Ulleberg, *Stand-alone power systems for the future: optimal design, operation and control of solar-hydrogen energy systems [Ph.D. thesis]*, Norwegian University of Science and Technology, 1998.

[10] K. Sapru, N. T. Stetson, S. R. Ovshinsky et al., "Development of a small scale hydrogen production-storage system for hydrogen applications," in *Proceedings of the 32nd Intersociety Energy Conversion Engineering Conference*, pp. 1947–1952, August 1997.

[11] H. Görgün, "Dynamic modelling of a proton exchange membrane (PEM) electrolyzer," *International Journal of Hydrogen Energy*, vol. 31, no. 1, pp. 29–38, 2006.

[12] H. J. N. Spruijt, D. M. O'Sullivan, and J. B. Klaassens, "PWM-switch modeling of DC-DC converters," *IEEE Transactions on Power Electronics*, vol. 10, no. 6, pp. 659–664, 1995.

[13] J. Chen, R. W. Erickson, and D. Maksimovic', "Averaged switch modeling of boundary conduction mode DC-to-DC converters," in *Proceedings of the 27th Annual Conference of the IEEE Industrial Electronics Society (IECON '01)*, vol. 2, pp. 844–849, Denver, Colo, USA, November 2001.

[14] A. Ammous, K. Ammous, M. Ayedi, Y. Ounajjar, and F. Sellami, "An advanced PWM-switch model including semiconductor device nonlinearities," *IEEE Transactions on Power Electronics*, vol. 18, no. 5, pp. 1230–1237, 2003.

[15] S. Abis, K. Ammous, H. Morel, and A. Ammous, "Advanced averaged model of PWM-switch operating in CCM and DCM conduction modes," *International Review of Electrical Engineering*, vol. 2, no. 4, pp. 544–556, 2007.